Spin and Pseudospin Symmetries in Λ Hypernuclei

LÜ Wanli, SUN Tingting†

(*School of Physics and Engineering, Zhengzhou University, Zhengzhou 450001, China*)

Abstract： Spin and pseudospin symmetries in the single-particle spectra of atomic nuclei are of great significance for the study of nuclear structure. In this work, taking ^{132}Sn, $^{133}_{\Lambda}$Sn, and $^{134}_{2\Lambda}$Sn as examples, the spin and pseudospin symmetries in Λ hypernuclei are studied by using the relativistic mean-field model. For the single-Λ spectra, results show that the spin symmetry maintains well while the pseudospin symmetry is approximately conserved. Besides, as impurities, the Λ hyperons worsen the spin symmetry of single-neutron spectra while improve the pseudospin symmetry.

Key words: spin symmetry; pseudospin symmetry; hypernuclei; impurity effect

1　Introduction

Symmetries in the single-particle (s.p.) spectra of atomic nuclei are of great importance on nuclear structure and have been extensively discussed in the literature (see Refs. [1–2] and references therein).

In ordinary nuclei, the single-particle spectra are characterized by an obvious violation of spin symmetry (SS) and an approximate pseudospin symmetry (PSS). The breaking of SS, *i.e.*, the remarkable spin-orbit (SO) splitting for the spin doublets $(n, l, j = l \pm 1/2)$ caused by the SO potential, lays the foundation to explain the traditional magic numbers in nuclear physics[3–4]. The conservation of PSS, *i.e.*, the quasi-degeneracy between two s.p. states with quantum numbers $(n, l, j = l + 1/2)$ and $(n - 1, l + 2, j = l + 3/2)$ redefined as the pseudospin doublets ($\tilde{n} = n$, $\tilde{l} = l + 1$, $j = \tilde{l} \pm 1/2$)[5–6], has been found related to a number of phenomena in nuclear structures, including deformation[7], superdeformation[8], magnetic moment[9], identical rotational bands[10–11], and so on.

Since the recognition of PSS in the nuclear spectrum, comprehensive efforts have been made to understand its origin. In 1997, Ginocchio pointed out that PSS is a relativistic symmetry in the Dirac Hamiltonian and becomes exact when the scalar and vector potentials satisfying $\Sigma(r) \equiv S(r) + V(r) = 0$[12]. He also revealed that the pseudo-orbital angular momentum $\tilde{l}$ is nothing but the orbital angular momentum of the lower component of the Dirac wave function[12]

and the occurrence of approximate PSS in nuclei is connected with certain similarities in the relativistic single-nucleon wave functions of the corresponding pseudospin doublets[13]. With a more general condition, Meng *et al.*[14–15] pointed out that $\mathrm{d}\Sigma(r)/\mathrm{d}r = 0$ can be approximately satisfied in exotic nuclei with highly diffuse potentials. They also related the onset of the pseudospin symmetry to a competition between the pseudo-centrifugal barrier (PCB) and the pseudospin-orbit (PSO) potential. Afterwards, the SS and PSS in nuclear spectra have been studied extensively such as PSS in the deformed nuclei[16–18], SS in anti-nucleon spectra[19–20], PSS in the s.p. resonate states[21–26], perturbative interpretation of SS and PSS[27–28], and PSS in supersymmetric quantum mechanics[29–31].

In hypernuclei, the studies of SS and PSS in the single-Λ spectra are also very important. Different from the single-nucleon spectra, experimentally, it has been found that the SO splittings for Λ hyperons are much smaller than that for nucleons. For example, the observed SO splitting of the p_{Λ} state in $^{13}_{\Lambda}$C is 0.152 ± 0.090 MeV, which is 20∼30 times smaller than that in ordinary nuclei[32]. Besides, since the first discovery of Λ hypernucleus in 1953[33], the study of hypernuclei has been attracting great interests of nuclear physicists[34–35]. One important goal of hypernuclear physics is to extract information on the baryon-baryon interactions including the strangeness of degree of freedom, which are crucial not only for hypernuclear structure[36–39] but also for neutron stars[40–44]. How-

ever, to our present knowledge, only few works on the SS in the anti-Λ spectra are performed[45–47]. Therefore, it is fascinating to study the SS and PSS in the single-Λ spectra. On the other side, since hyperons do not suffer from the nucleon's Pauli exclusion principle, there will be a series of responses for the nuclear core if any hyperons penetrate into the nuclear interior as an impurity. Thus, it is also very interesting to study the impurity effects from hyperons on the nuclear SS and PSS.

During the past decades, the relativistic mean-field (RMF) model has achieved great successes not only in ordinary nuclei[48–50] but also in hypernuclei[51–55]. The relativistic approach is suitable for the discussion of SO splittings, as the SO interaction naturally emerges within the relativistic framework. Adopting the RMF model, there are many works on SS and PSS[2], which have achieved great successes.

In this work, the SS and PSS in single-Λ spectra are studied within the framework of RMF model. The impurity effects from Λ hyperons on the nuclear SS and PSS symmetries are also discussed. The paper is organized as follows. In Sec. 2, we present the RMF model for Λ hypernuclei and the formalism of SS and PSS in the single-Λ spectrum. After the numerical details introduced in Sec. 3, we present the results and discussions in Sec. 4. Finally, a summary is given in Sec. 5.

2 Theoretical framework

The starting point of the meson-exchange RMF model for Λ hypernuclei is the covariant Lagrangian density

$$\mathcal{L} = \mathcal{L}_\mathrm{N} + \mathcal{L}_\Lambda, \tag{1}$$

where $\mathcal{L}_\mathrm{N}$ is the standard RMF Lagrangian density for nucleons[49], and $\mathcal{L}_\Lambda$ represents the contribution from hyperons[52]. Since Λ hyperons are charge neutral and isoscalar, only the couplings with the σ- and ω-meson are included in $\mathcal{L}_\Lambda$, i.e.,

$$\mathcal{L}_\Lambda = \bar{\psi}_\Lambda \Big[\mathrm{i}\gamma^\mu \partial_\mu - m_\Lambda - g_{\sigma\Lambda}\sigma - g_{\omega\Lambda}\gamma^\mu \omega_\mu - \frac{f_{\omega\Lambda\Lambda}}{2m_\Lambda}\sigma^{\mu\nu}\partial_\nu \omega_\mu \Big]\psi_\Lambda, \tag{2}$$

where m_Λ is the mass of the Λ hyperon, $g_{\sigma\Lambda}$ and $g_{\omega\Lambda}$ are respectively the coupling constants with the σ- and ω-meson, and the last term is the $\omega\Lambda\Lambda$ tensor coupling introduced due to small SO splitting of hyperons[56].

Starting from the Lagrangian density (1) and with the mean-field and no-sea approximations, the s.p. Dirac equations for baryons and the Klein-Gordon equations for mesons and photon can be obtained by the variational procedure.

To study the SS and PSS in the s.p. spectrum with the RMF theory, we will examine the Dirac equations governing the motion of baryons. In the spherical case, the Dirac spinor for Λ hyperons can be expanded as

$$\psi_{n\kappa m}(\boldsymbol{r}) = \frac{1}{r}\left(\begin{array}{c} \mathrm{i}G_{n\kappa}(r)Y^l_{jm}(\theta,\phi) \\ -F_{\tilde{n}\kappa}(r)Y^{\tilde{l}}_{jm}(\theta,\phi) \end{array} \right), \tag{3}$$

where $G_{n\kappa}(r)/r$ and $F_{\tilde{n}\kappa}(r)/r$ are the upper and lower components of the radial wave functions with n and $\tilde{n}$ numbers of radial nodes, $Y^l_{jm}(\theta,\phi)$ is the spinor spherical harmonic, $\tilde{l} = l - \mathrm{sign}(\kappa)$ is pseudo-orbital angular momentum, and the quantum number κ is defined as $\kappa = (-1)^{j+l+1/2}(j+1/2)$.

With the radial wave functions, the Dirac equation for the Λ hyperon can be written as,

$$\left(\begin{array}{cc} V+S & -\dfrac{\mathrm{d}}{\mathrm{d}r}+\dfrac{\kappa}{r}+T \\ \dfrac{\mathrm{d}}{\mathrm{d}r}+\dfrac{\kappa}{r}+T & V-S-2m_\Lambda \end{array} \right)\left(\begin{array}{c} G \\ F \end{array} \right) = \varepsilon\left(\begin{array}{c} G \\ F \end{array} \right), \tag{4}$$

with the s.p. energy ε and the mean-field scalar potential S, vector potential V, and tensor potential T,

$$S = g_{\sigma\Lambda}\sigma, \quad V = g_{\omega\Lambda}\omega_0, \quad T = -\frac{f_{\omega\Lambda\Lambda}}{2m_\Lambda}\partial_r\omega_0. \tag{5}$$

Here and hereafter, the subscript κ is omitted for simplification. To compare the SS and PSS symmetries of single-Λ spectra with those of single-nucleon spectra, the tensor potential is omitted in this paper. Its effects on the SS and PSS of Λ hyperons can be referred to Ref. [57].

Starting from the Dirac equation (4), one can go a step further and get a second-order Schrödinger-like equation for either the upper or the lower component. To study the SS, we will analyze the Schrödinger-like equation for the upper component G, and to study the PSS, we will analyze that for the lower component F.

For the upper component G, one can obtain

$$\left\{ -\frac{1}{M_+}\frac{\mathrm{d}^2}{\mathrm{d}r^2} + \frac{1}{M_+^2}\frac{\mathrm{d}M_+}{\mathrm{d}r}\frac{\mathrm{d}}{\mathrm{d}r} + V + S + \frac{1}{M_+}\cdot \frac{\kappa(\kappa+1)}{r^2} + \frac{1}{M_+^2}\frac{\mathrm{d}M_+}{\mathrm{d}r}\frac{\kappa}{r} \right\}G = \varepsilon G, \tag{6}$$

with the energy-dependent effective mass $M_+ = \varepsilon + 2m_\Lambda - V + S$. In analogy with the Schrödinger equation, $V+S$ is the central potential; the term proportional to $\kappa(\kappa+1) = l(l+1)$ corresponds to the centrifugal barrier (CB); and the last term corresponds to the SO potential leading to the substantial SO splitting in the s.p. spectrum. Namely,

$$V_{\mathrm{CB}}(r) = \frac{1}{M_+}\frac{\kappa(\kappa+1)}{r^2}, \tag{7a}$$

$$V_{\mathrm{SO}}(r) = \frac{1}{M_+}\left(\frac{1}{M_+}\frac{\mathrm{d}M_+}{\mathrm{d}r} \right)\frac{\kappa}{r}. \tag{7b}$$

It is well known that there is no SO splitting if the potential V_{SO} vanishes, *i.e.*, $\frac{\mathrm{d}M_+}{\mathrm{d}r} = -\frac{\mathrm{d}(V-S)}{\mathrm{d}r} = 0$ corresponds to the SS limit. Note that this condition is equivalent to the mean-field potentials $V-S=0$ in the whole r space if they go to zero at infinity.

For the lower component $F(r)$, one can obtain

$$\left\{ -\frac{1}{M_-}\frac{\mathrm{d}^2}{\mathrm{d}r^2} + \frac{1}{M_-^2}\frac{\mathrm{d}M_-}{\mathrm{d}r}\frac{\mathrm{d}}{\mathrm{d}r} + V - S - 2m_\Lambda + \frac{1}{M_-} \cdot \right.$$
$$\left. \frac{\kappa(\kappa-1)}{r^2} - \frac{1}{M_-^2}\frac{\mathrm{d}M_-}{\mathrm{d}r}\frac{\kappa}{r} \right\}F = \varepsilon F, \qquad (8)$$

with the energy-dependent effective mass $M_- = \varepsilon - V - S$. The term in the above equation proportional to $\kappa(\kappa-1) = \tilde{l}(\tilde{l}+1)$ is regarded as the PCB and the last term corresponds to the PSO potential, which leads to the substantial PSO splitting. Namely,

$$V_{\text{PCB}}(r) = \frac{1}{M_-}\frac{\kappa(\kappa-1)}{r^2}, \qquad (9a)$$

$$V_{\text{PSO}}(r) = -\frac{1}{M_-}\left(\frac{1}{M_-}\frac{\mathrm{d}M_-}{\mathrm{d}r} \right)\frac{\kappa}{r}. \qquad (9b)$$

If the potential V_{PSO} vanishes, there is no PSO splitting, *i.e.*, $\frac{\mathrm{d}M_-}{\mathrm{d}r} = \frac{\mathrm{d}(V+S)}{\mathrm{d}r} = 0$ corresponds to the PSS limit. Note that this condition is equivalent to the mean-field potentials $V+S=0$ in the whole r space if they go to zero at infinity.

3　Numerical details

In this work, (hyper)nuclei ^{132}Sn, $^{133}_{\Lambda}$Sn, and $^{134}_{2\Lambda}$Sn are taken as examples to study the SS and PSS in Λ hypernuclei. For the NN interaction, the parameter set PK1[58] is adopted. For the ΛN interaction, the scalar coupling constant $g_{\sigma\Lambda}/g_{\sigma\text{N}} = 0.618$ is constrained by reproducing the experimental binding energies of Λ hyperon in the $1s_{1/2}$ state of hypernucleus $^{40}_{\Lambda}$Ca[59]; the vector coupling constant $g_{\omega\Lambda}/g_{\omega\text{N}} = 0.666$ is determined according to the naive quark model[60]. Here, $g_{\sigma\text{N}}$ and $g_{\omega\text{N}}$ are the coupling constants between nucleons and σ- and ω-meson in the Lagrangian $\mathcal{L}_{\text{N}}$, respectively. With these NN and ΛN interactions, the single-Λ spectra of hypernuclei ranging from $^{12}_{\Lambda}$C to $^{208}_{\Lambda}$Pb can be described well[59]. The Dirac equation (4) in the RMF model is solved in the coordinate space with a box size of $R = 20$ fm and a step size of 0.05 fm.

4　Results and discussion

In Fig. 1, the calculated single-Λ spectra and the mean-field potential in $^{133}_{\Lambda}$Sn are presented. In the upper panel, six sets of spin doublets are displayed, *i.e.*, $1p$ ($1p_{1/2}$ and $1p_{3/2}$), $1d$ ($1d_{3/2}$ and $1d_{5/2}$), $1f$ ($1f_{5/2}$ and $1f_{7/2}$), $1g$ ($1g_{7/2}$ and $1g_{9/2}$), $2p$ ($2p_{1/2}$ and $2p_{3/2}$), and $2d$ ($2d_{3/2}$ and $2d_{5/2}$). Almost all these spin doublets are found to be quasi-degenerate. We can see that the splitting of spin doublets with the same principal quantum number increases with the angular momentum l increasing, which is because the centrifugal barrier $V_{\text{CB}} = \frac{1}{M_+}\frac{l(l+1)}{r^2}$ keeps the particle away from the center so that a big overlap between the wave function $G(r)$ and the spin-orbit potential always happens for larger l[61]. This has been observed in single-Λ states in $^{89}_{\Lambda}$Y by the (π^+, K^+) reactions at KEK[32]. In the lower panel, four sets of pseudospin doublets are exhibited, *i.e.*, $1\tilde{p}$ ($1d_{3/2}$ and $2s_{1/2}$), $1\tilde{d}$ ($1f_{5/2}$ and $2p_{3/2}$), $1\tilde{f}$ ($1g_{7/2}$ and $2d_{5/2}$), and $2\tilde{p}$ ($2d_{3/2}$ and $3s_{1/2}$). For the deeply bound doublets $1\tilde{p}$ ($1d_{3/2}$ and $2s_{1/2}$) and $1\tilde{d}$ ($1f_{5/2}$ and $2p_{3/2}$), the splittings are large. However, for the less bound $1\tilde{f}$ ($1g_{7/2}$ and $2d_{5/2}$) and $2\tilde{p}$ ($2d_{3/2}$ and $3s_{1/2}$) doublets near the threshold, the PSS is preserved very well, especially for the $2\tilde{p}$ doublets, which are almost degenerate. Note that for the $\tilde{s}_{1/2}$ states with $\tilde{l} = 0$, they have no pseudospin partners. From above discussions, the spin symmetry maintains considerably well for almost all the spin doublets while the pseudospin symmetry is approximately conserved in the single-Λ spectra of $^{133}_{\Lambda}$Sn.
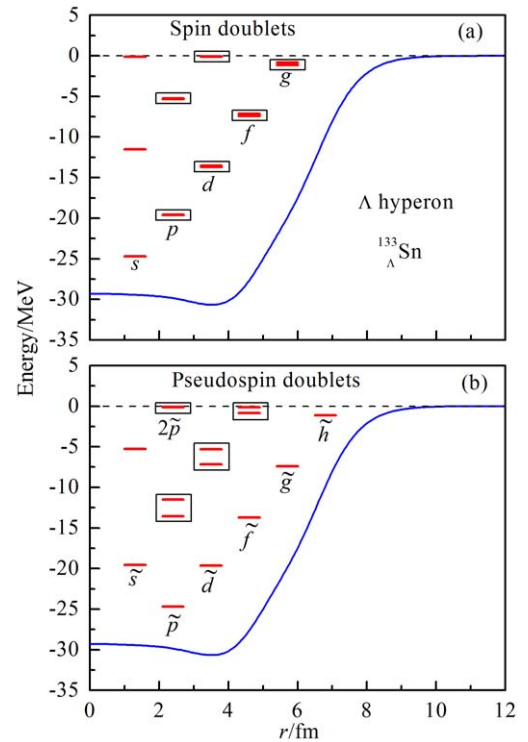

Fig. 1　(color online) Single-Λ spectra in $^{133}_{\Lambda}$Sn. Upper: spin doublets; Lower: pseudospin doublets. Each pair of doublets is marked by a box.

In order to show the SO and PSO splittings more clearly, the reduced SO splittings $\Delta E_{\text{SO}} = (\varepsilon_{j_<} -$

$\varepsilon_{j_>})/(2l+1)$ and reduced PSO splittings $\Delta E_{\mathrm{PSO}} = (\varepsilon_{j_<} - \varepsilon_{j_>})/(2\tilde{l}+1)$ versus the average s.p. energies $E_{\mathrm{av}} = (\varepsilon_{j_<} + \varepsilon_{j_>})/2$ are respectively plotted in the upper and lower panels of Fig. 2. For the spin doublets, all the energy splittings are less than 0.1 MeV, which are much smaller than those in single-nucleon spectra. This can be understood from Eq. (7b), where the SO splitting V_{SO} for hyperons is reduced when compared to that for nucleons due to a larger effective mass M_+ in the denominator or the larger Λ-hyperon mass m_Λ compared to the nucleon mass and due to the smaller couplings to σ- and ω-meson. Besides, SS for Λ hyperons are less energy dependent, which is also caused by the large Λ-hyperon mass m_Λ in the effective mass $M_+ = \varepsilon + 2m_\Lambda - V + S$, where $2m_\Lambda$ is much larger than either the potential $S-V$ or the s.p. energy ε. For the pseudospin doublets, however, obvious energy dependence can be seen. For the $1\tilde{p}$ doublets, the reduced PSO splitting is 0.67 MeV, but almost vanishes for the $2\tilde{p}$ doublets. The PSS in the single-Λ spectra is quite similar to that in the single-nucleon spectra.
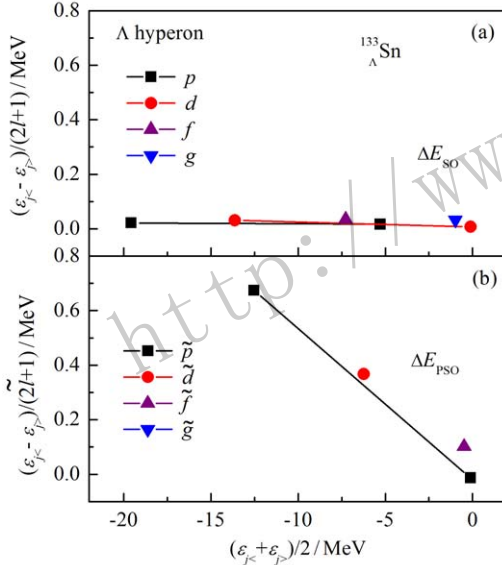

Fig. 2 (color online) (a) Reduced SO splitting $\Delta E_{\mathrm{SO}} = (\varepsilon_{j_<} - \varepsilon_{j_>})/(2l+1)$ and (b) reduced PSO splitting $\Delta E_{\mathrm{PSO}} = (\varepsilon_{j_<} - \varepsilon_{j_>})/(2\tilde{l}+1)$ versus their average s.p. energies $E_{\mathrm{av}} = (\varepsilon_{j_<} + \varepsilon_{j_>})/2$ for Λ hyperon in $^{133}_{\Lambda}$Sn. For spin doublets, $j_< = l - 1/2$ and $j_> = l + 1/2$; for pseudospin doublets, $j_< = \tilde{l} - 1/2$ and $j_> = \tilde{l} + 1/2$. Spin (pseudospin) doublets with the same l ($\tilde{l}$) are linked by lines.

To analyze the mechanism of the SS and PSS in the single-Λ spectrum shown in Figs. 1 and 2, we compare the centrifugal barrier $V_{\mathrm{CB}}(r)$ with spin-orbit potential $V_{\mathrm{SO}}(r)$ and the pseudo-centrifugal barrier $V_{\mathrm{PCB}}(r)$ with pseudospin-orbit potential $V_{\mathrm{PSO}}(r)$. Here we only show the results of pseudospin doublets, because the results of spin doublets can be analyzed

analogously. It was pointed out in Ref. [14] that if

$$\left| V_{\mathrm{PSO}}(r) \right| \ll \left| V_{\mathrm{PCB}}(r) \right|, \tag{10}$$

the pseudospin symmetry will be good. However, unfortunately, it is difficult to compare them directly, as potentials $V_{\mathrm{PSO}}(r)$ and $V_{\mathrm{PCB}}(r)$ in Eq. (9) have a singularity at $M_-(r) = 0$. Since we are only interested in the relative magnitude, the effective PCB and the effective PSO potentials,

$$V_{\mathrm{PCB}}^{\mathrm{eff}}(r) = M_-(r) \frac{\kappa(\kappa - 1)}{r^2}, \tag{11a}$$

$$V_{\mathrm{PSO}}^{\mathrm{eff}}(r) = -\frac{\mathrm{d} M_-(r)}{\mathrm{d} r} \frac{\kappa}{r}, \tag{11b}$$

are introduced by multiplying a factor of $M_-^2(r)$ in Eq. (9). In Eq. (11), the effective PCB and PSO potentials do not depend on the s.p. energy.

In Fig. 3, the comparison of the PCB with PSO potential for the $1\tilde{p}$ and $2\tilde{p}$ pseudospin doublets of the Λ hyperon in hypernucleus $^{133}_{\Lambda}$Sn are presented, respectively. From Fig. 3, the effective PCB is much bigger than the effective PSO potential in the coordinate space with $r < 5$ fm, which leads to the approximate PSS. However, around the nuclear surface with $r > 5$ fm, the effective PSO is bigger than the effecitve PCB. The effective PCB for $1\tilde{p}$ doublets are smaller than that for $2\tilde{p}$ doublets, which has the consequence that the PSS is much better for the weakly bound pseudospin doublets.
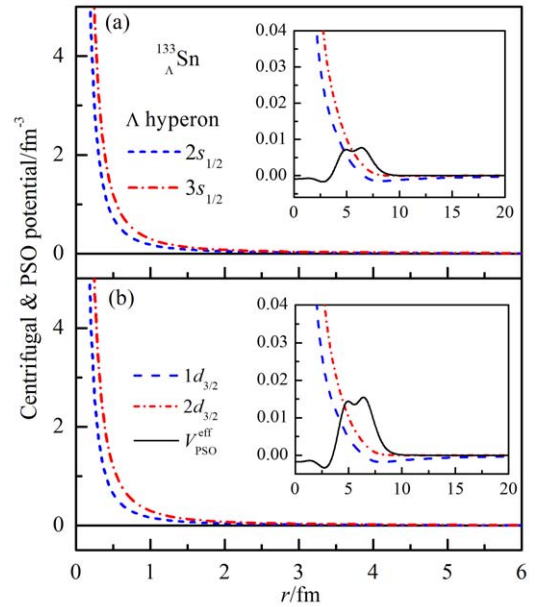

Fig. 3 (color online) Comparison of the Λ hyperon effective PCB $V_{\mathrm{PCB}}^{\mathrm{eff}}$ (dashed and dot-dashed lines) and the effective PSO potential $V_{\mathrm{PSO}}^{\mathrm{eff}}$ (solid lines) for the (a) $s_{1/2}$ and (b) $d_{3/2}$ states in $^{133}_{\Lambda}$Sn. The dashed lines are for $2s_{1/2}$ and $1d_{3/2}$ states, and the dot-dashed lines are for $3s_{1/2}$ and $2d_{3/2}$ states.

Finally, the impurity effects of Λ hyperons on SS and PSS in the single-neutron spectrum are discussed. In Fig. 4, taking ^{132}Sn, $^{133}_{\Lambda}$Sn, and $^{134}_{2\Lambda}$Sn as examples, the spin-orbit splittings ΔE_{SO} and the pseudospin-orbit splittings ΔE_{PSO} versus the average s.p. energies E_{av} are plotted in the upper and lower panels, respectively. For SS, with increasing the number of Λ hyperons, the energy splittings between all the spin doublets become larger. Namely, adding more Λ hyperons makes SS in the single-neutron spectrum worse. However, a complete reversal of trend is observed for the pseudospin doublets. That is, with the increasing number of Λ hyperons, ΔE_{PSO} decreases and makes PSS better in the single-neutron spectrum. This impurity effect results from the modification of the PCB and PSO when Λ hyperons appear and further discussions can be seen in Ref. [62].
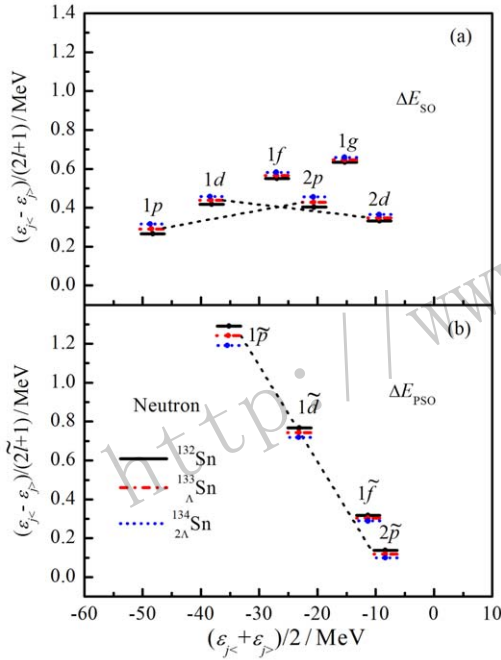

Fig. 4　(Color online) Reduced spin-orbit splittings ΔE_{SO} (a) and reduced pseudospin-orbit splittings ΔE_{PSO} (b) versus their average s.p. energies E_{av} (the midpoints) for the single-neutron spectra of ^{132}Sn, $^{133}_{\Lambda}$Sn, and $^{134}_{2\Lambda}$Sn.

5　Summary

In this work, the SS and PSS in the Λ hypernuclei are studied within the framework of RMF theory.

Taking hypernucleus $^{133}_{\Lambda}$Sn as an example, the SS and PSS in the single-Λ spectra are studied. Well conserved SS are found, which is in consistent with experimental results of the small SO splitting, but different from the breaking of SS in the single-nucleon spectrum. However, PSS in the single-Λ spectrum is approximately conserved, which is quite similar as that in single-nucleon spectrum. To understand the mechanism of such behaviors of the (P)SS in the single-Λ spectrum, comparison of the (P)CB with the (P)SO potentials of single-Λ states are performed. We find that PCB is much larger than the PSO with $r < 5$ fm but smaller with $r > 5$ fm, which leads to approximate PSS.

Besides, taking ^{132}Sn, $^{133}_{\Lambda}$Sn, and $^{134}_{2\Lambda}$Sn as examples, the impurity effects of Λ hyperons on SS and the PSS in the single-neutron spectrum have been investigated. Adding more Λ hyperons makes SS worse while makes PSS better. This impurity effect results from the modification of the PCB and PSO when Λ hyperons appear.

References:

[1]　GINOCCHIO J N. Phys Rep, 2005, **414**: 165.
[2]　LIANG H Z, MENG J, ZHOU S G. Phys Rep, 2015, **570**: 1.
[3]　MAYER M G. Phys Rev, 1949, **75**: 1969.
[4]　HAXEL O, JENSEN J H D, SUESS H E. Phys Rev, 1949, **75**: 1766.
[5]　HECHT K T, ADLER A. Nucl Phys A, 1969, **137**: 129.
[6]　ARIMA A, HARVEY M, SHIMIZU K. Phys Lett B, 1969, **30**: 517.
[7]　BOHR A, HAMAMOTO I, MOTTELSON B R. Phys Scr, 1982, **26**: 267.
[8]　DUDEK J, NAZAREWICZ W, SZYMANSKI Z, *et al.* Phys Rev Lett, 1987, **59**: 1405.
[9]　NAZAREWICZ W, TWIN P J, FALLON P, *et al.* Phys Rev Lett, 1990, **64**: 1654.
[10]　BYRSKI T, BECK F A , CURIEN D, *et al.* Phys Rev Lett, 1990, **64**: 1650.
[11]　ZENG J Y, MENG J, WU C S, *et al.* Phys. Rev. C, 1991, **44**: R1745.
[12]　GINOCCHIO J N. Phys Rev Lett, 1997, **78**: 436.
[13]　GINOCCHIO J N, MADLAND D G. Phys Rev C, 1998, **57**: 1167.
[14]　MENG J, SUGAWARA-TANABE K, YAMAJI S, *et al.* Phys Rev C, 1998, **58**: R628.
[15]　MENG J, SUGAWARA-TANABE K, YAMAJI S, *et al.* Phys Rev C, 1999, **59**: 154.
[16]　LALAZISSIS G A, GAMBHIR Y K, MAHARANA J P, *et al.* Phys Rev C, 1998, **58**: R45.
[17]　SUGAWARA-TANABE K, ARIMA A. Phys Rev C, 1998, **58**: R3065.
[18]　GINOCCHI J N, LEVIATAN A, MENG J, *et al.* Phys Rev C, 2004, **69**: 034303.
[19]　ZHOU S G, MENG J, RING P. Phys Rev Lett, 2003, **91**: 262501.
[20]　HE X T, ZHOU S G, MENG J, *et al.* Eur Phys J A, 2006, **28**: 265.
[21]　GUO J Y, WANG R D, FANG X Z. Phys Rev C, 2005, **72**: 054319.
[22]　ZHANG S S, SUN B H, ZHOU S G. Chin Phys Lett, 2007,

24: 1199.

[23] LU B N, ZHAO E G, ZHOU S G. Phys Rev Lett, 2012, **109**: 072501.

[24] LU B N, ZHAO E G, ZHOU S G. Phys Rev C, 2013, **88**: 024323.

[25] LU B N, ZHAO E G, ZHOU S G. AIP Conf Proc, 2013, **1533**: 63.

[26] LU B N, ZHAO E G, ZHOU S G. J Phys: Conf Ser, 2014, **533**: 012021.

[27] LISBOA R, MALHEIRO M, ALBERTO P, et al. Phys Rev C, 2010, **81**: 064324.

[28] ALBERTO P, FIOLHAIS M, MALHEIRO M, et al. Phys Rev C, 2002, **65**: 034307.

[29] LEVIATAN A. Phys Rev Lett, 2004, **92**: 202501.

[30] LIANG H Z, SHEN S H, ZHAO P W, et al. Phys Rev C, 2013, **87**: 014334.

[31] SHEN S H, LIANG H Z, ZHAO P W, et al. Phys Rev C, 2013, **88**: 024311.

[32] AJIMURA S, HAYAKAWA H, KISHIMOTO T, et al. Phys Rev Lett, 2001, **86**: 4255.

[33] DNAYSZ M, PNIEWSKI J. Philos Mag, 1953, **44**: 348.

[34] HASHIMOTO O, TAMURA H. Prog Part Nucl Phys, 2006, **57**: 564.

[35] GAL A, HUNGERFORD E V, MILLENER D J. Rev Mod Phys, 2016, **88**: 035004.

[36] MA Z Y, SPETH J, KREWALD S, et al. Nucl Phys A, 1996, **608**: 305.

[37] HIYAMA E, MOTOBA T, RIJKEN T A, et al. Prog Theor Phys Suppl, 2010, **185**: 1.

[38] LIU Z X, XIA C J, LU W L, et al. Phys Rev C, 2018, **98**: 024316.

[39] SUN T T, HIYAMA E, SAGAWA H, et al. Phys Rev C, 2016, **94**: 064319.

[40] HOFMANN F, KEIL C M, LENSKE H. Phys Rev C, 2001, **64**: 025804.

[41] SCHAFFNER-BIELICH J. Nucl Phys A, 2008, **804**: 309.

[42] VIDANA I. Nucl Phys A, 2013, **914**: 367.

[43] SUN T T, XIA C J, ZHANG S S, et al. Chin Phys C, 2018, **42**: 025101.

[44] XIA C J, PENG G X, SUN T T, et al. Phys Rev D, 2018, **98**: 034031.

[45] SONG C Y, YAO J M, MENG J. Chin Phys Lett, 2009, **26**: 122102.

[46] SONG C Y, YAO J M. Chin Phys C, 2010, **34**: 1425.

[47] SONG C Y, YAO J M, MENG J. Chin Phys Lett, 2011, **28**: 092101.

[48] MENG J, TOKI H, ZHOU S G, et al. Prog Part Nucl Phys, 2006, **57**: 470.

[49] MENG J, ZHOU S G. J Phys G: Nucl Part Phys, 2015, **42**: 093101.

[50] SUN T T. Sci Sin-Phys Mech Astron, 2016, **46**: 012006. (in Chinese)

[51] BROCKMANN R, WEISE W. Phys Lett B, 1977, **69**: 167.

[52] MARES J, JENNINGS B K. Phys Rev C, 1994, **49**: 2472.

[53] LU B N, ZHAO E G, ZHOU S G. Phys Rev C, 2011, **84**: 014328.

[54] LU B N, HIYAMA E, SAGAWA H, et al. Phys Rev C, 2014, **89**: 044307.

[55] XIA H J, MEI H, YAO J M. Sci Sin-Phys Mech Astron, 2017, **60**: 102021.

[56] JENNINGS B. Phys Lett B, 1990, **246**: 325.

[57] SUN T T, LU W L, ZHANG S S. Phys Rev C, 2017, **96**: 044312.

[58] LONG W H, MENG J, GIAI N VAN, et al. Phys Rev C, 2004, **69**: 034319.

[59] REN S H, SUN T T, ZHANG W. Phys Rev C, 2017, **95**: 054318.

[60] DOVER C B, GAL A. Prog Part Nucl Phys, 1984, **12**: 171.

[61] MENG J, TANIHATA I. Nucl Phys A, 1999, **650**: 176.

[62] LU W L, LIU Z X, REN S H, et al. J Phys G: Nucl Part Phys, 2017, **44**: 125104.

Λ 超核中单粒子谱的自旋及赝自旋对称性研究

吕万里，孙亭亭†

(郑州大学物理工程学院；郑州 450001)

摘要： 原子核中单粒子谱的自旋和赝自旋对称性对核结构的研究具有重要意义。本文基于相对论平均场理论，以 ^{132}Sn，$^{133}_{\Lambda}$Sn，及 $^{134}_{2\Lambda}$Sn 为例，研究了 Λ 超核中单 Λ 谱和单中子谱的自旋和赝自旋对称性。研究发现，单 Λ 谱的自旋对称性保持得相当好，与实验观测一致；而其赝自旋对称性只是近似保持，与核子谱的情况类似。此外，还研究了 Λ 超子对中子谱的杂质效应，发现 Λ 超子使中子谱的自旋对称性变差，赝自旋对称性变好。

关键词： 自旋对称性；赝自旋对称性；超核；杂质效应